

Estimation of fracture toughness of cast steel container from Charpy impact test data

Tassadit Bellahcene^a and Meziane Aberkane^{*}

Laboratoire d'Elaboration, de Caractérisation des Matériaux et Modélisation (LEC2M), Université Mouloud Mammeri de Tizi-Ouzou, BP 17 RP, Tizi-Ouzou, 15008, Algeria

(Received June 7, 2016, Revised July 25, 2017, Accepted August 10, 2017)

Abstract. Fracture energy values KV have been measured on cast steel, used in the container manufacture, by instrumented Charpy impact testing. This material has a large ductility on the upper transition region at $+20^{\circ}\text{C}$ and a ductile tearing with an expended plasticity before a brittle fracture on the lower transition region at -20°C . To assess the fracture toughness of this material we use, the K_{IC} - KV correlations to measure the critical stress intensity factor K_{IC} on the lower transition region and the dynamic force - displacement curves to measure the critical fracture toughness $J_{\rho C}$, the essential work of fracture Γ_e on the upper transition region. It is found, using the K_{IC} - KV correlations, that the critical stress intensity factor K_{IC} remains significant, on the lower transition region, which indicating that our testing material preserves his ductility at low temperature and it is apt to be used as a container's material. It is, also, found that the J_{ρ} - ρ energetic criterion, used on the upper transition region, gives a good evaluation of the fracture toughness closest to those found in the literature. Finally, we show, by using the Γ_e - K_{IC} relation, on the lower transition region, that the essential work of fracture is not suitable for the toughness measurement because the strong scatter of the experimental data. To complete this study by a numerical approach we used the ANSYS code to determine the critical fracture toughness J_{ANSYS} on the upper transition region.

Keywords: Charpy impact test; fracture toughness; ductility; upper transition region; lower transition region

1. Introduction

Design of containers against the risk of brittle fracture by shock requires to measure dynamic fracture toughness values. To ensure structural integrity and assure continued or extended life of the structure a fracture safe analysis is done using fracture mechanics principle usually, Linear Elastic Fracture Mechanics LEFM. LEFM analysis requires exact evaluation of material fracture toughness K_{IC} . To measure K_{IC} , a rapid and cheap method consists to use Charpy specimen because its simplicity.

The Charpy test is still a very popular toughness test, although the measured quantity, the fracture

energy KV , is known to be strongly dependant on specimen geometry, size, notch sharpness and loading rate. Therefore, the fracture energy of the standard specimen has neither a direct relation to the fracture toughness in terms of K_{IC} or J_{IC} . The physical processes involved are rather different. For these reasons KV rather serves as an "indicating" than a "quantifying" toughness parameter. Nevertheless, fracture toughness is often estimated from KV . A number of corresponding K_{IC} - KV correlations are offered in the literature (Teran *et al.* 2016, Berdin and Prioul 2007, Qamar *et al.* 2006, Kim *et al.* 2002, Bannister 1998, Kapp and Underwood 1992, Barthelemy 1980). It is,

also, possible, when the material has a large ductility, to use elastic-plastic fracture mechanics based J -integral techniques for the determination of fracture toughness value (Hohe *et al.* 2015, Sreenivasan 2014). The J_C assessment consists in calculating the J -integral from the energy consumed at the point of unstable fracture (instability load point), which may be preceded by plastic deformation. The J_C testing is based only on determination of the total energy values. The standardised procedure to determine J_C needs precracked specimens, which is a costly and time-consuming procedure. On the other hand, there are situations where the precracking fatigue of a specimen is not feasible. It, then, becomes possible to use the toughness J_C as a function of notch radius ρ . Using Rice expression, Landes and Begley (Akouri *et al.* 2000) have calculated the toughness J_C as a function of notch radius from load-displacement curves. Their results show that the fracture toughness increases linearly with the notch root radius ρ . Based on the (Srinivas and Kamat 1992) and (Firrao and Robert 1983) works, Akouri *et al.* (2000) show that if we take into consideration the effect of the notch root radius we obtain two phases of evolution of the fracture toughness with notch radius ρ : in the first one, it remains constant and equal to J_C as a function of notch radius until a critical value ρ_C of the notch radius is reached where in the second phase J_C as a function of notch radius increases linearly with ρ : If the effect of the notch root radius is neglected, the fracture toughness increases linearly also with the notch root radius ρ : The difference between the results given in the two points above can reach the value of the fracture toughness. Another, practical method overcomes the detection of the

*Corresponding author, Professor

E-mail: aberkane_meziane@ummto.dz

^aPh.D.

Table 1 Relation between K_{IC} and KV on upper transition region

	Relation between K_{IC} [MPa \sqrt{m}] and KV [J]	Equation number	Validity domain	
			KV [J]	σ_e [MPa]
Rolfe and Barsom (Qamar <i>et al.</i> 2008)	$\left(\frac{K_{IC}}{\sigma_e}\right)^2 = 0,646 \frac{KV}{\sigma_e} - 6,35 \times 10^{-3}$	(1)		
Brite-Euram Sintap (Bannister 1998)	$K_{IC} = 0,54KV + 55$	(2)	>60	
Kapp and Underwood (1992)	$\left(\frac{K_{IC}}{\sigma_e}\right)^2 = 0,52 \left(\frac{KV}{\sigma_e} - 0,02\right)$	(3)		

Table 2 Relation between K_{IC} and KV on lower transition region

Authors	Relation between K_{IC} [MPa \sqrt{m}] and KV [J]	Equation number	Validity domain	
			KV [J]	σ_e [MPa]
Rolfe and Barsom (Berdin and Prioul 2007)	$K_{IC} = 6,76(KV)^{3/4}$	(4)	4-82	270-1700
Sailors and Cortens (Berdin and Prioul 2007)	$K_{IC} = 14,6(KV)^{1/2}$	(5)	2.7-61	250-345
Brite-Euram Sintap (Bannister 1998)	$K_{IC} = \left[(K_{mat_{25}} - 20)(25/B)^{1/4} \right] + 20$ $K_{mat_{25}} = 12\sqrt{KV} \quad (B=25 \text{ mm})$	(6)		
Marandet and Sanz (Berdin and Prioul 2007)	$K_{IC} = 19(KV)^{1/2}$ $TK_{IC} = 9 + 1,37TK_{28}$ $K_{IC} = 20 + (11 +$	(7)	5-110	274-820
Wallin (Berdin and Prioul 2007)	$77 \exp(0,019(T - TK_{28} + 18))$ $\times (25/B)^{1/4} \times (\ln(1 - P_F))^{1/4}$ $TK_{IC} = TK_{28}$	(8)		

crack initiation is the essential work of fracture (EWF). The EWF is equivalent to the critical J -integral value (Rink *et al.* 2014, Tuba *et al.* 2013). In comparison with the well-established J -integral method, the main attraction of the EWF is its experimental simplicity. In the EWF approach, one only needs to measure the ligament length before testing rather than measuring the crack extension as required in the J -integral method.

In this paper, estimation of the fracture toughness of cast steel container from impact test data was investigated. In the first part, some of the older and newer Charpy-fracture toughness KV - K_{IC} correlations have been examined and used to calculate the critical stress intensity factor K_{IC} on the lower transition zone and on the upper transition region respectively. In the second part, by using the dynamic force-displacement curves which are obtained by an instrumented Charpy impact test machine, we calculate by two energetic methods, detailed in the following, the material toughness. This work is, finally, completed by a numerical study using ANSYS code which allows to plot the stress concentration curves on the notch and to determine the critical fracture toughness J_{ANSYS} on the upper transition region.

2. A brief literature background

2.1 Measure of the critical stress intensity factor K_{IC} on notched specimens connecting to the fracture energy KV

As mentioned previously, the Charpy test provides essentially a qualitative characterization of materials to the rough fracture (Brnic *et al.* 2014). The results of the Charpy test are not directly usable for a quantitative approach of the damage as it can be developed by the fracture mechanics. This quantitative approach requires knowledge of the K_{IC} toughness of the material, but the fracture energy KV measured by Charpy test and toughness K_{IC} can not be connected in a simple way. Several fundamental differences between the two measures should be highlighted:

- The toughness K_{IC} is the value of the stress intensity factor for a crack which becomes unstable. The stress intensity factor is a global parameter characterizing the local stress field at the crack tip.
- The fracture energy KV is a global setting. This energy is the sum of the plastic and the fracture energies. The Charpy test sample is not being pre cracked and a part of energy is used to initiate cracking.

Nevertheless many K_{IC} - KV correlations have been proposed to evaluate the toughness K_{IC} from the fracture energy KV determined by Charpy test. Most of these correlations are only valid in a restricted temperature domain and are defined in a narrow range of mechanical properties. Two types of approaches can be distinguished, the simplest correlations, such as those proposed by Rolfe and Barsoms, Sailors and Cortens, Kapp and Underwood and Brite Euram Sintap based on a direct passage between the two variables (Barthelemy 1980, Bannister 1998, Berdin

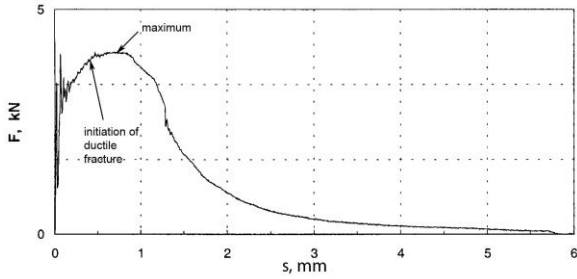


Fig. 1 Instrumented Charpy impact test force-displacement curve in upper transition region region; (Cast steel, test temperature +20°C. velocity 5.50 m/s)

and Prioul 2007, Kapp and Underwood 1992, Kim *et al.* 2002). Others, more sophisticated, take account of brittle - ductile transition shift of temperature. This is the case of the formulation proposed by Marandet and Sanz and Wallin (Berdin and Prioul 2007).

2.2 The Different correlation between K_{IC} and KV

Due to the shape of the Charpy transition curve, there is no single correlation which can be used for the lower transition region and upper transition region areas. The decision as to which correlation to be used therefore depends on the type of the data available, the likely Charpy behaviour of the material at the design operating temperature and the nature the estimate required. Two basic correlation approaches are described in this paper:

- On the upper transition region
- On the lower transition region

For (1), three expressions are given. For (2), five correlations are given. All the literature correlations used in this paper are consigned in Table 1 and Table 2.

K_{IC} is the critical intensity factor in mode I of fracture, σ_e the yield limit, B is the specimen thickness, KV is the impact strength and TK28 is defined as the temperature corresponding to $KV=32$ J (Bannister 1998). E the young's Modulus equal to 2.1×10^5 MPa. P_F is the cumulative failure probability

$$P_F = 1 - \exp \left[- \left(\frac{K_C - K_{\min}}{K_0 - K_{\min}} \right)^m \right] \quad (9)$$

K_C is the fracture toughness, K_0 is equal to the value of K_C which represents the failure probability of 0,63, m is the Weibull slope, for cleavage fracture was known to be 4 and K_{\min} is known to be about $20MPa\sqrt{m}$ for ferritic steel (Kim *et al.* 2002).

2.3 The fracture criteria based on the energy consumed at the point of unstable fracture.

It is, also, possible to characterize the toughness by the fracture energetic methods like the J -integral and the essential work of fracture on the upper transition region and on the lower transition region respectively by using the force versus time-displacement diagrams obtained by the

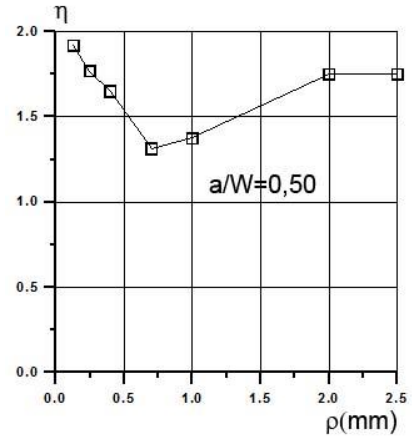


Fig. 2 Evolution of η versus notch radius ρ for constant relative notch depth $a/W=0.50$ (Charpy U-notched specimen)

instrumented impact tests. Several approaches for correlations between the J -integral and the Charpy upper transition region and the Charpy lower transition region energies have been proposed in the literature (Hohe *et al.* 2015, Sreenivasan 2014, Schindler and Veidt 1998, Schindler and Bertschinger 2002).

2.3.1 The fracture toughness on the upper transition region

On the upper transition region, the fracture is ductile (Lucon 2016) and the force versus time diagram obtained from the instrumented impact test is shown in Fig. 1.

The J -integral is conventionally defined for non-linear elastic material as path independent line integral and can be used in this case because the large ductility of the material before a brittle fracture. Although ASME E813-87 and ASTM E1152-87 apply only to ductile fracture. More recent standard permit J testing of materials those fails in a brittle manner (Pettarin *et al.* 2006). The J_C assessment consists in calculating the J -integral from the energy consumed at the point of unstable fracture (instability load point) which may or may not be preceded by plastic deformation or very little slow crack growth. The inherent J_C testing - based only on direct determination of the total energy value of a set of similar samples - makes it very attractive method. The standardised procedure to determine J_C needs precracked specimens, which is a costly and time-consuming procedure. On the other hand, there are situations where the precracking fatigue of a specimen is not feasible. It, then, becomes possible to use the toughness J_C as a function of notch radius ρ . The J_C parameter as defined, here, provided that the specimens used are single-edge notched three-point-bending specimens with a constant crack to deep ratio $a/W=0.5$ and different notch radius ρ varying between 0.13 mm and 2 mm. Using this test samples (Aberkane *et al.* 2001, Pluvinage 2007) it is shown that it is possible to measure graphically the critical fracture toughness value $J_{\rho C}$ on a J_{ρ} versus ρ curve by extrapolation. For each couple of $a/W=0.5$ and ρ the total area under the load-deflection curve U_{tot} is measured and divided by the ligament area for determining J_{ρ} .

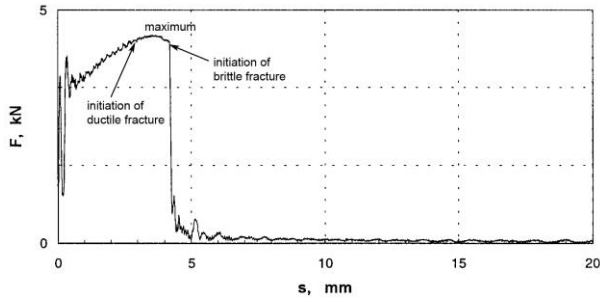


Fig. 3 Instrumented Charpy impact test force-displacement curve on the lower transition region (cast steel. test temperature -20°C . velocity 5.5 m/s)

$$J_{\rho} = \frac{\eta U_{tot}}{B(W-a)} \quad (10)$$

η is a parameter characterizing the notch radius influence on the fracture energy (Akouri *et al.* 2000). It is computed by finite element using stress strain behaviour as described by Ludwik law. Fig. 2 shows the evolution of η for constant relative notch depth $a/W=0,50$ versus notch radius ρ . The solutions of $a/W=0.5$ for each value of ρ are deduced about Fig. 2 and introduced in Eq. (10).

The J_{ρ} works done for the different notch radius versus their correspondent notch radius values ρ are drawing on a diagram and $J_{\rho C}$ fracture toughness can be obtained by a graphic interpolation.

2.3.2 The fracture toughness on the lower transition region

On the lower transition region, where the force versus time diagram is shown in Fig. 3.

We can observe that the unstable cleavage fracture occurs after some amount stable tearing. The suitable fracture energy in this case, when the ductile tearing is the principle fracture mode can be the essential work of fracture considering the small specimen dimensions and the large ductility of the material. This method is interesting because it does not require the detection of the crack initiation. In this method it has been suggested that the non elastic region at the tip of a notches may be divided into an end region, where the fracture process take place, and an outer region, where screening plastic deformation is necessary to accommodate the large strains in the end region (Fig. 4).

The end region work initiates the crack and is termed the essential work of fracture U_e and the outer region work which is responsible for plastic deformation is termed U_{pl} . The total fracture work is therefore written as

$$U_t = U_e + U_{pl} \quad (11)$$

The total specific work of fracture or the work of fracture per unit ligament area may be written as

$$\frac{U_t}{(W-a)B} = \Gamma_e + \psi(W-a)W_{pl}^* \quad (12)$$

Γ_e is the specific essential is work of fracture, W_{pl}^* is

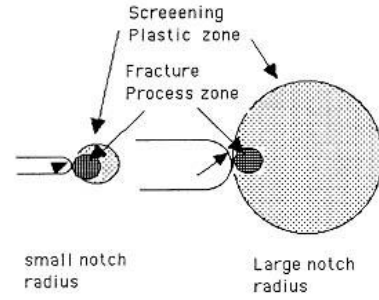


Fig. 4 Schematic of the relative size of the fracture process zone and the screening plastic zone for small and large notch radius

Table 3 Chemical composition

Weight %	C	Si	Mn	Cr	Mo	Ni	Cu
Cast steel	0.09	0.37	1.18	0.12	0.03	0.29	0.29

Table 4 Mechanical properties

Yield stress σ_e (MPa)	Ultimate strength UTS (MPa)	A%
375	478	31.7

the specific plastic work of fracture. $(W-a)$ is the ligament length. B is the specimen thickness and ψ is a shape factor which describes the size of the plastic zone According to the above equation. A straight-line relationship exists between the specific work of fracture and the ligament length and Γ_e can be obtained when $(W-a)$ is extrapolated to zero.

3. Material and experimental procedure

3.1 Material

The investigated steel material is a cast steel. The chemical composition and the mechanical properties are given in Table 3 and in Table 4 respectively.

We assume that the material is strain hardening and obeys the following stress-strain law

$$\sigma = K\varepsilon^n \quad (13)$$

Where K is the strain-hardening coefficient and n the strain-hardening exponent ($K=737$ MPa; $n=0.12$).

3.2 Specimens and experimental procedure

Charpy specimens made of cast steel oriented perpendicular to rolling direction were tested. The dynamic tests were carried out in a standard impact machine equipped with an instrumented tup. The impact velocity of the tup is 5.50 m/s. dynamic three-point bend tests on standard Charpy V-notched specimens (ASTM E23 Charpy Impact testing) were performed in a large temperature range, -80°C to $+40^{\circ}\text{C}$ with a geometry specimen given in Fig. 5.

To measure the fracture toughness by the J_{ρ} - ρ method and the essential work of fracture on the upper transition

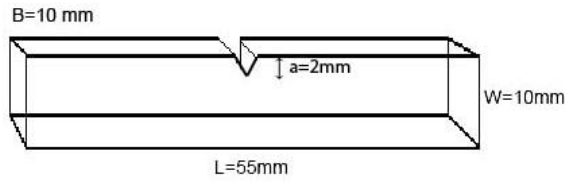


Fig. 5 The Charpy-V specimen

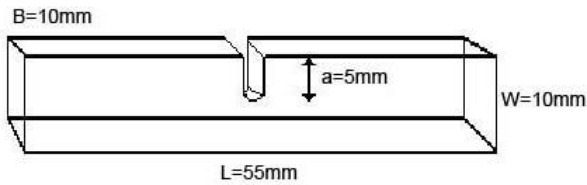
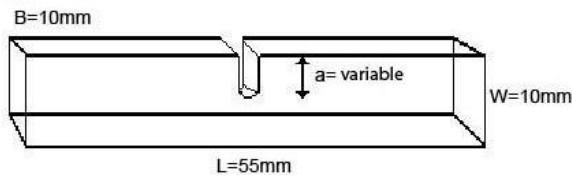

 Fig. 6 The Charpy-U specimen used on the upper transition region ($T=+20^{\circ}\text{C}$)

 Fig. 7 The Charpy-U specimen used on the lower transition region ($T=-20^{\circ}\text{C}$)

 Table 5 Geometry of the different Charpy U-notched specimens with a constant relative notch depth $a/W=0,5$ used on the upper transition region ($T=+20^{\circ}\text{C}$)

a/W	0.5						
ρ (mm)	0.13	0.25	0.4	0.7	1	2	2.5

 Table 6 Geometry of the different Charpy U-notched specimens with a constant notch radius $\rho=0.7$ mm used on the lower transition region ($T=-20^{\circ}\text{C}$)

ρ (mm)	0.7						
a (mm)	2	3	4	5	6	7	
$b_0=W-a$ (mm)	8	7	6	5	4	3	

region and on the lower transition region respectively we use Charpy-U notched specimens (ISO 148-1 U-Notch pendulum testing) with the dimensions described in Figs. 6-7 and Tables 5-6.

4. Experimental results and discussion

4.1 The brittle-ductile transition curve

Impact tests were carried out on a temperature range comprising between -80°C and $+40^{\circ}\text{C}$. These tests permitted to draw a brittle-ductile transition curve of the cast steel material used in our tests. We can, observe on this curve a middle scatter ($R\text{-squared}=0,84$) of the experimental data due to the nature of the impact tests. All these Charpy impact test results are consigned in Table 7 and represented in Fig. 8.

Table 7 The Charpy's impact test results

Temperature test [$^{\circ}\text{C}$]	Measured value of KV [J]	Fitted value of KV [J]
20	KV=181	KV=139
	KV=136	
	KV=100	
0	KV=98	KV=69
	KV=40	
-20	KV=56	KV=42
-40	KV=28	KV=14
	KV=14	
-60	KV=8	KV=7
	KV=6	
-80	KV=16	KV=12
	KV=8	

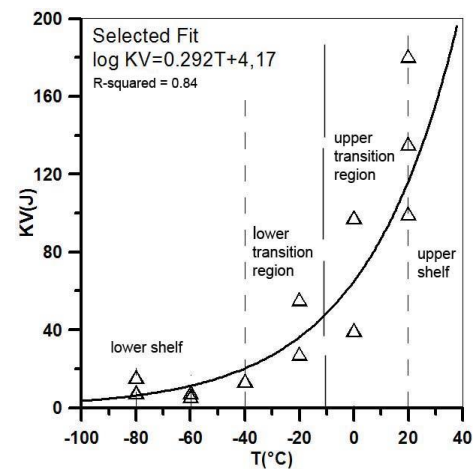


Fig. 8 The brittle-ductile transition curve

 Table 8 The SIF critical values determined in the upper transition region $T=+20^{\circ}\text{C}$

Used methods	Rolf-Barsom	Brite Euram Sintap	Kapp-Underwood
Fitted Impact Toughness KV [J]	139	139	139
Critical SIF K_{IC} [$\text{MPa}\sqrt{\text{m}}$]	181	130	160

4.2 Toughness values

4.2.1 The critical stress intensity factor K_{IC}

The critical SIF values are calculated on the upper transition region at $T=+20^{\circ}\text{C}$ and on the lower transition region at $T=-20^{\circ}\text{C}$ by the equations done on table 1 and table 2 respectively. The values of KV for $T=+20^{\circ}\text{C}$ and $T=-20^{\circ}\text{C}$, used in these different equations, are those given by the fitted values consigned on Table 7. The calculated critical SIF values are presented in Tables 8-9.

These tables show that K_{IC} toughness on the upper transition region is greater than that one on the lower transition region. Fracture toughness increases with increase of temperature. These results are agree with the Teran *et al.* 2016 ones which found, that there is no single fracture toughness value even at a fixed temperature and loading rate. These tables show, also, that the Rolf-Barsom toughness values are always greater and that the Brite-

Table 9 The SIF critical values determined in the lower transition region $T=-20^{\circ}\text{C}$

Used methods	Rolfe-Barsom	Sailors-Cortens	Brite-Euram Sintap	Marandet-Sanz
Fitted Impact Toughness KV [J]	42	42	42	32
Critical SIF K_{IC} [$MPa\sqrt{m}$]	111.5	94.7	92.6	107.5

Table 10 The $U/B(W-a)$ values determining for their correspondent a values

$a=2$ [mm]	$a=3$ [mm]	$a=4$ [mm]	$a=5$ [mm]	$a=6$ [mm]	$a=7$ [mm]
$(W-a)=8$	$(W-a)=7$	$(W-a)=6$	$(W-a)=5$	$(W-a)=4$	$(W-a)=3$
$U/B(W-a)$ [J/mm ²]					
0,8900	0,94071429	0,42016667	0,5152	0,44025	0,51533333
0,438875	0,327	0,74116667	0,492	0,2575	0,449
0,491625	0,61471429	0,3205	0,4254	0,69925	0,27533333
0,744625	0,264	0,468	0,4456	0,3485	0,19
0,70375	0,42214286	0,23016667	0,1828	0,5075	0,63366667

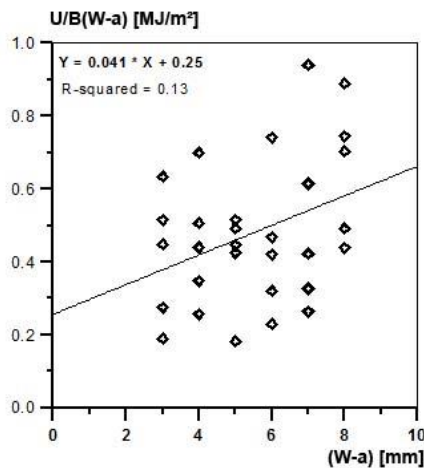


Fig. 9 Variation of $U/B(W-a)$ versus the ligament size $(W-a)$

Euram Sintap (BES) toughness values are always lower. This indicating that the BES's toughness values seem to be the more conservative ones and that the BES (K_{IC} -KV) correlations promote the material safety. We observe, also, that the BES's toughness values are close to those of the literature (Barthelemy 1980, Bannister 1998). On the other size, we can see that the fracture toughness value remains significant on the lower transition region, as compared to this of the upper transition region which indicating that our testing material seems to preserve his ductility, even, at low temperature.

4.2.2 The essential work of fracture Γ_e criterion on the lower transition region

All the $U/B(W-a)$ energy values for each ligament size $(W-a)$ used in this study are regrouped in Table 10.

In the following, we plot the $U/B(W-a)$ specific energies values with there corresponding length ligament $(W-a)$.

Table 11 The critical SIF K_{IC} determined with Γ_e value

Used methods	Lower transition region ($T=-20^{\circ}\text{C}$)
Fracture toughness Γ_e [MJ/m^2]	0,25
Equivalent Critical SIF K_{IC} [$MPa\sqrt{m}$] with relation (15)	229

Table 12 Review of the calculated critical SIF K_{IC} on the lower transition region ($T=-20^{\circ}\text{C}$)

Used methods	Rolfe-Barsom	Sailors-Cortens	Brite-Euram Sintap	Marandet-Sanz	Equivalent K_{IC} via Γ_e method
Fitted Impact Toughness KV [J]	42	42	42	32	
Critical SIF K_{IC} [$MPa\sqrt{m}$]	111.5	94.7	92.6	107.5	229

Extrapolation to origin gives the value of the essential work for fracture. It is equal to 0.25 MJ/m^2 . We observe on this figure a strong scatter (R -squared=0,13). The large scatter of fracture toughness data in the transient region has been reported by Kim *et al.* (2002) and it is due to the great effect of the specimen thickness on the fracture toughness data. The fracture toughness can either be determined using large specimen satisfying linear-elastic requirements or it can be derived from the elastic-plastic energy J -integral value corresponding to brittle fracture with the following equation

$$K_{IC} = \sqrt{J_C E} \tag{14}$$

E is the Young's modulus it is equal to $2,1 \times 10^5$ MPa for the cast steel, J_C is the critical energy consumed at the point of unstable fracture he has the same mean of Γ_e , so we can re-write Eq. (14) like

$$K_{IC} = \sqrt{\Gamma_e E} \tag{15}$$

By using the Γ_e determined in paragraph 4.2.2, we can calculate the value of an equivalent K_{IC} from Eq. (15).

All the critical SIF K_{IC} [$MPa\sqrt{m}$] values on the lower transition region ($T=-20^{\circ}\text{C}$) are regrouped in a Table 12.

This table let us to observe that the energy criterion (Γ_e method) gives the highest toughness values in comparison to the K_{IC} -KV correlations. This value is due to the value of Γ_e which it is not reliable due to the large scatter of the experimental data. This indicates that in the lower transition region, despite an appreciable material plasticity due to ductile tearing before an unstable cleavage fracture, the specific essential work of fracture Γ_e is not suitable to determine a critical value of toughness. In this region the K_{IC} -KV correlations seem to give a good evaluation of fracture toughness, comparatively to those of the literature, especially the BES's toughness value.

4.2.3 The J_{pC} criterion on the upper transition region

All the values of J_p , F_{\max} the maximum force on the upper transient region force-displacement curves for each notch radius ρ used in this study are regrouped in Table 13.

Table 13 The J_{ρ} values determined for there corresponding notch radius ρ

$\rho=0.13$ [mm]	$\rho=0.25$ [mm]	$\rho=0.40$ [mm]	$\rho=0.7$ [mm]	$\rho=1$ [mm]	$\rho=2$ [mm]	$\rho=2.5$ [mm]
$\eta=1.92$	$\eta=1.77$	$\eta=1.65$	$\eta=1.313$	$\eta=1.375$	$\eta=1.75$	$\eta=1.75$
$J_{\rho} = \frac{\eta U}{Bb}$						
[MJ/m ²]						
0,2288	0,1787	0,1783				
0,1912	0,1411	0,11428	0,1253	0,1778	0,3020	0,2885
0,1496	0,1310	0,1513	0,1337	0,1691	0,2503	0,2410
0,1,647	0,1514	0,1787	0,1300	0,1418	0,2793	0,2913
0,1393	0,1833	0,1904	0,0990	0,1829	0,3104	
F_{max} [kN]						
5,317	5,415	5,365	5,154			
5,318	4,9	5,31	5,464	5,266	5,398	5,289
4,77	4,738	5,022	4,948	5,337	5,283	5,141
4,86	5,089	5,219	4,57	5,685	5,436	5,312
4,711	5,034	5,471	5,505		5,389	

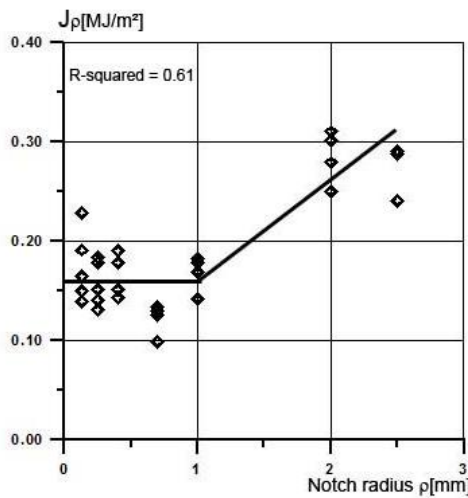


Fig. 10 J_{ρ} versus there corresponding notch radius ρ

The J_{ρ} versus the notch radius ρ graph (Fig. 10) is plotted according to Table 13.

This graph shows that the majority of the experimental data are concentrating on a plateau starting at $\rho=0.13$ mm and ending at $\rho=1$ mm. The scattering of the experimental data is moderate on this plateau (R -squared=0,61). Beyond this upper limit ($\rho=1$ mm) the J_{ρ} values increase appreciably until $\rho=2$ mm and it stabilizes at $\rho=2.5$ mm. The critical value of J_{ρ} called $J_{\rho C}$ is then determined by extrapolating on the J_{ρ} axis zero and it is equal to $J_{\rho C}=0,16$ MJ/m² and the limit of this plateau $\rho_C=1$ mm is defined, here, as the critical notch radius. The existence of a critical notch root radius below which fracture toughness is independent of ρ has been reported by several authors (Akkouri *et al.* 2000, Srinivas and Kamat 1992, Firrao and Robert 1983, Mourad *et al.* 2013, Chaudhari *et al.* 2009, Mourad and El-Domiatiy 2011). Akkouri *et al.* (2000) concluded that the dependence of the fracture toughness for ductile steel on the notch radius has been obtained if they take into consideration the effect of the notch root radius on the η factor, then, they obtained two phases of evolution of the fracture toughness with notch radius: in the first one, it

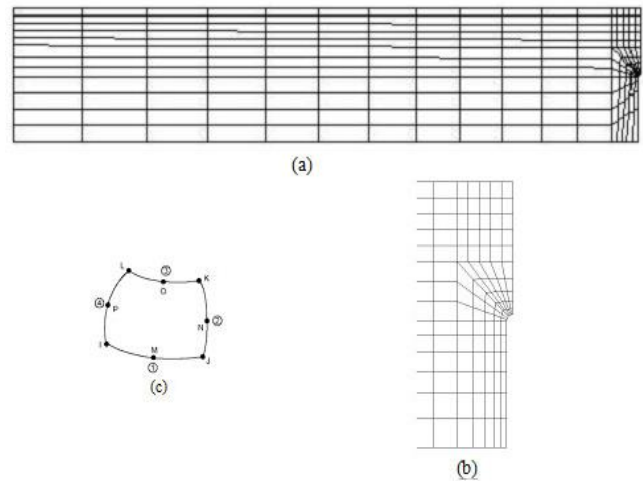


Fig. 11 (a) The finite element mesh in half of the specimen. (b) The finite element meshes of the notch (c) finite element mesh

remains constant and equal to J_{IC} until a critical value of the notch radius is reached where in the second phase J_{IC} increases linearly with ρ . The value of $J_{\rho C}$ is closest to those of the literature for different steels these critical values named J_L, J_W by P.R. Sreenivassen (2014) was situated between 0,125MJ÷0,145 MJ/m² for E460 steel tested at 20°C and J_i values equal to 0,135 MJ/m² for an RPV steel (Schmitt *et al.* 1994) and J_{IC} value equal to 0,120MJ/m² for an A-533B pressure vessel material (Nilsson and Östenson 1978).

4.2.4 Determination of the material toughness on the upper transition region by numerical simulations

Finite element modelling

An analysis using the finite element model in ANSYS code is presented in this section. Figs. 11(a)-11(b) show the geometry of the Charpy specimen mesh. Due to symmetry of the problem, a half model can be used. The finite element mesh consists, on quadrilateral elements (quadratic) with eight (08) nodes automatically generated (Fig. 11(c)). The

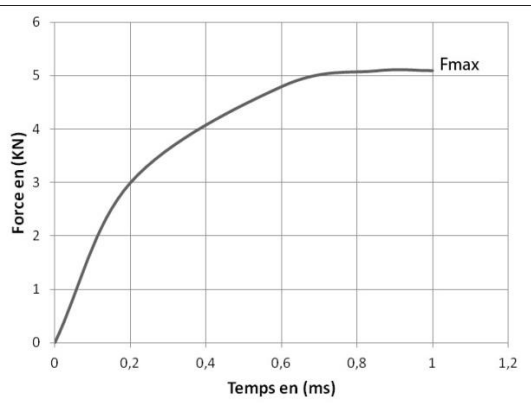


Fig. 12 Applied impulse loading

Table 14 Values of maximum forces F_{max} recorded in the tests for each notch radius ρ (Table 13) and the numerical J_{ANSYS}

$\rho=0.25$ [mm]	$\rho=0,40$ [mm]	$\rho=0.7$ [mm]	$\rho=1$ [mm]	$\rho=1$ [mm]	$\rho=1$ [mm]
F_{max} [kN]	F_{max} [kN]	F_{max} [kN]	F_{max} [kN]		
5,034	5,022	4,57	5,266	5,283	5,141
5,415	5,471	5,505	5,685	5,436	5,312
J_{ANSYS} [MJ/m ²]					
0,2183	0,2314	0,2106	0,2430	0,2434	0,2369
0,2495	0,2520	0,2537	0,2750	0,2505	0,2448

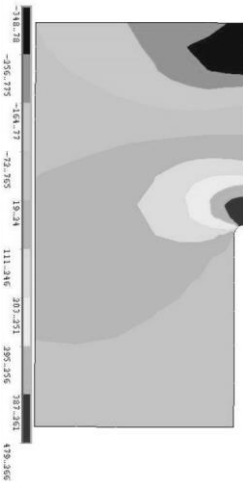


Fig. 13(a) $F_{max}=5,089$ kN; $\rho=0,25$ mm

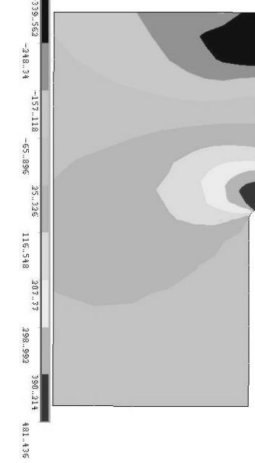


Fig. 13(b) $F_{max}=5,415$ kN; $\rho=0,25$ mm

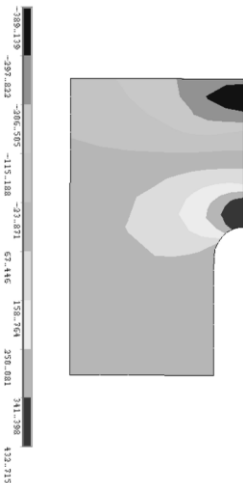


Fig. 13(c) $F_{max}=5,266$ kN; $\rho=1$ mm

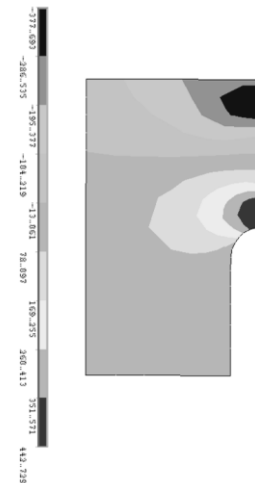


Fig. 13(d) $F_{max}=5,685$ kN; $\rho=1$ mm

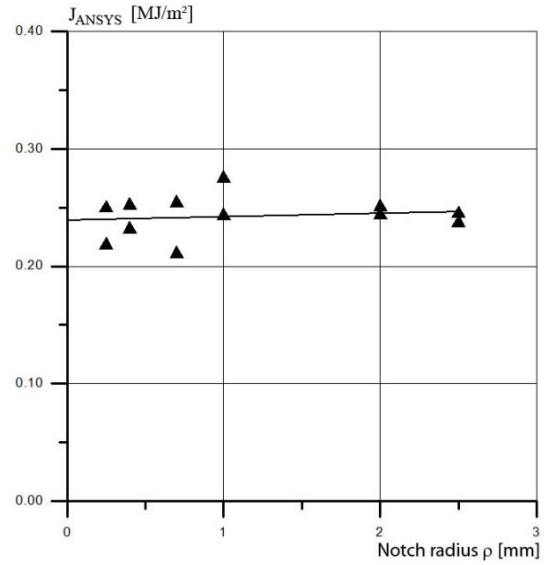


Fig. 14 numerical J_{ANSYS} versus notch radius ρ

number of nodes is about 431 nodes and the number of elements is about of 1390 elements. The mesh is finer when we approach the bottom of the notch.

Impact simulation

The Charpy impact test are simulated with a time-dependant loads applied on duration of 1ms from $F=0$ to

$F=F_{max}$ on the on the opposite face to the notched specimen. F_{max} is the peak load value, identified by the Charpy tests.

The transient dynamic analysis is used and the calculations are carried out using the Full Method (ANSYS 2016, Bathe 1996). The exact material stress-strain data are inserted into the computation and material strain hardening is included. Fully dynamic analyses have only been carried out in 2-D, since dynamic computation in 3-D is very costly Rossol *et al.* (1999). J -integral around the notch which is equal to the change in the potential energy and evaluated with the ANSYS workbench containing fracture module which evaluates J -integral directly (Witts 2005).

Numerical results

For different geometries we determined the stress concentration at $F=F_{max}$ and we present it in these following figures.

These figures show that the notched face is the tensile area and the opposite face is the most compressed one and this was expected. We observe, also, that the tensile stress concentrations values are biggest in the notched area when the notched radius is the smaller. J -integral results from the post-processor were obtained by using the nonlinear isotropic material option in ANSYS. The computed values of J -integral J_{ANSYS} , for each notch radius, are calculated. There values are listed in Table 14.

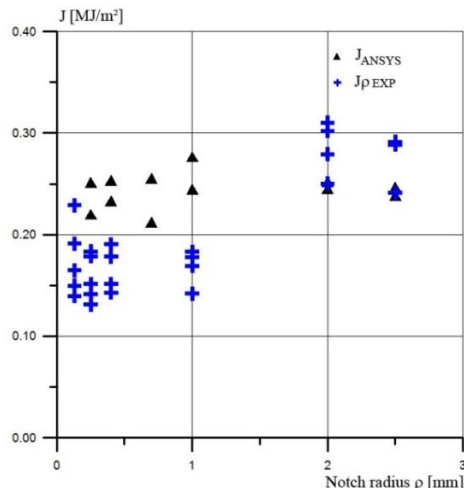


Fig. 15 A comparison between experimental data versus Ansys

In the following, we plot the variation of numerical J_{ANSYS} as a function of the notch radius ρ .

Fig. 14 shows a linear relationship between the J_{ANSYS} values and notch radius ρ . The numerical critical fracture toughness $J_{C\text{ANSYS}}$ can be determined by extrapolation of the linear curve and it is equal to 2,4 MJ/m². This value is greatest than the experimental one. The difference between the experimental and numerical fracture toughness J_{ANSYS} (Fig. 15) is due to the non taking into account, in the numerical calculation, of the notch radius influence characterized by the parameter η . This fact have been reporting by Akkouri *et al.* (2000), which acknowledges that when the effect of the notch root radius on η is neglected, the fracture toughness J increases linearly also with the notch root radius ρ . This numerical study, confirm the importance of the notch radius influence in the fracture toughness calculus. On the other side, The fracture toughness was calculated from the dynamic finite element analysis by using a postprocessor it calculate not only those parts of the fracture toughness derived from the mechanical stresses and strains, but also to include additional parts arising from thermal strains and dynamic masses (Rossoll *et al.* 1999), which seems explain the difference between J_{pC} and the numerical fracture toughness $J_{C\text{ANSYS}}$ Eberle, Klingbeil and Schiker (2000), seen that the above a certain value, of crack extension in the ligament, they observe that the calculated J overestimates slightly the experimental values.

5. Conclusions

This work presents an estimation of fracture toughness from instrumented Charpy impact testing on cast steel. On the upper transition region, fracture toughness is determined using the K_{IC} -KV correlations, the $J_{p-\rho}$ energetic criterion and a finite elements calculation with ANSYS code. On the lower transition region fracture toughness is determined using the K_{IC} -KV correlations and the essential work of fracture energetic criteria. Based on the results of this study,

the following conclusions are made:

- On the upper transition region the $J_{p-\rho}$ energetic criterion gives a good evaluation of the toughness closest to these found in the literature.
- The essential work of fracture is not suitable for the toughness determination of the material in the lower shelf because the strong scatter of the experimental points.
- In term of fracture toughness values the K_{IC} -KV correlations are more conservative than the energetic criteria.
- The numerical computation, confirm the literature conclusions which state that when the effect of the notch root radius on η is neglected, the fracture toughness increases linearly also with the notch root radius ρ .

This study leads us to conclude that it is possible to use the Charpy instrumented test as a toughness method with a good accuracy and a cheap cost. We can, also, conclude that the cast steel used in our tests is apt to be used as a container's material because his ductility and his good toughness at a low temperature (-20°C).

References

- Aberkane, M., Lenkey, G.Y.B. and Pluvinage, G. (2001) "Dynamic fracture toughness of cast steel used for nuclear waste containers with notched charpy specimen", *Transactions SMIRT 16*, Washington DC, August.
- Akourri, O., Louah, M., Kifani, A., Gilgert, G. and Pluvinage, G. (2000), "The effect of notch radius on fracture toughness JIC", *Eng. Fract. Mech.*, **65**, 491-505.
- ANSYS (2016), <http://www.ansys.stuba.sk>
- Bannister, A.C. (1998), "Determination of fracture toughness from charpy impact energy: procedure and validation", Sub-Task 3.3 Report. No SINTAP/BS/17; British Steel plc, Swinden Technology Centre Moorgate, Rotherham S60 3AR, United Kingdom.
- Barthelemy, B. (1980), *Notions Pratiques De La Mécanique De La Rupture*, (Practical concepts of fracture mechanics), Lavoisier Edition, France.
- Bathe, K.J. (1996), *Finite Element Procedures*, Prentice-Hall, Englewood Cliffs, New Jersey.
- Berdin, C. and Prioul, C. (2007), "Relation résilience-ténacité-apports de la modélisation numérique", (Fracture energy-toughness relationship- contributions of numerical modeling) Document m4168-Techniques de l'ingénieur, Paris, France
- Brnic, J., Turkalj, G. and Canadija, M. (2014), "Mechanical testing of the behavior of steel 1.7147 at different temperatures", *Steel Compos. Struct.*, **17**(5), 549-560.
- Chaudhari, V.V., Kulkarn, D.M. and Prakash, R. (2009), "Study of influence of notch root radius on fracture behaviour of extra deep drawn steel sheets", *Fatigue Fract. Eng. Mater. Struct.*, **32**, 975-86
- Eberle, A., Klingbeil, D. and Schicker, J. (2000), "The calculation of dynamic Jr-curves from the finite element analysis of a Charpy test using a rate-dependent damage model", *Nucl. Eng. Des.*, **198**, 75-87.
- Firrao, R. and Robert, R. (1983), "Ductile fracture nucleation ahead of sharp cracks", *Metall. Sci. Technol.*, **1**, 5-13.
- Hohe, J., Siegle, D., Bechler, E. and Nagel, G. (2015), "Standard and customized correlation of crack resistance curves and charpy shelf energy for german reactor pressure vessel steels", *Int. J. Pres. Ves. Pip.*, **134**, 101-111.

- Kapp, J.A. and Underwood, J.I.L. (1992), "Correlation between fracture toughness, charpy v-notch impact energy, and yield strength for astm a723 steel", Memorandum report ARCCB-MR-92008, US Army Armament Research, Development and Engineering Center, New York, USA.
- Kim, S.H., Park, Y.W., Kang, S.S. and Chung, H.D. (2002), "Estimation of fracture toughness transition curve of rpv steels from charpy impact test data", *Nucl. Eng. Des.*, **212**, 49-57.
- Lucon, E. (2016), "Estimating dynamic ultimate tensile strength from instrumented Charpy data", *Mater. Des.*, **97**, 437-443.
- Mourad, A.H.I and EL-Domiatiy, A. (2011), "Notch radius and specimen size effects on fracture toughness of low alloy steel", *Procedia Eng.*, **10**, 1348-1353.
- Mourad, A.H.I., El-Domiatiy, A. and Chao, Y.J. (2013), "Fracture toughness prediction of low alloy steel as a function of specimen notch root radius and size constraints", *Eng. Fract. Mech.*, **103**, 79-93.
- Nilsson, F. and Östensson, B. (1978), " J_{IC} -testing of A-533 B statistical evaluation of some different testing techniques", *Eng. Fract. Mech.*, **10**(2), 223-232.
- Pettarin, V., Elicabe, G.E., Frontini, P.M., Leskovic, K., Lenkey, G.Y.B. and Czigan, T. (2006), "Analysis of low temperature impact fracture data of thermoplastic polymers making use of an inverse methodology", *Eng. Fract. Mech.*, **73**, 738-749.
- Pluinage, G. (2007), *Fracture and Fatigue Emanating from Stress Concentrators*, Springer Science et Business Media, Dordrecht, Netherland.
- Qamar, S.Z., Sheikh, A.K., Arif, A.F.M. and Pervez, T. (2006) "Regression-based CVN-KIC models for hot work tool steels", *Mater. Sci. Eng. A*, **430** (1-2), 208-215.
- Rink, M., Andena, L. and Marano, C. (2014), "The essential work of fracture in relation to J-integral", *Eng. Fract. Mech.*, **127**, 46-55.
- Rossoll, A., Berdin, C., Forget, P., Prioul, C. and Marini, B. (1999), "Mechanical aspect of the Charpy impact test", *Nucl. Eng. Des.*, **188**, 217-229.
- Schindler, H.J. and Bertschinger, P. (2002), "Relation of fracture energy of sub-sized Charpy specimens to standard Charpy energy and fracture toughness", Transferability of Fracture Mechanical Characteristics, Edited by Ivo Dlouhy, NATO Sciences Series, 213-224.
- Schindler, H.J. and Veidt, M. (1998), "Fracture toughness evaluation from instrumented sub-size charpy-type tests", *Small Spec. Test Techniq.*, ASTM STP, **1329**, 48-61.
- Schmitt, W., Sun, D.Z., Böhme, W and Nagel, G. (1994), "Evaluation of fracture toughness based on results of instrumented Charpy tests", *Int. J. Pres. Ves. Pip.*, **59**, 21-29
- Sreenivasan, P.R. (2014), "Estimation of quasi-static J_r -curves from charpy energy and adaptation to asme e 1921 reference temperature estimation of ferritic steels", *Nucl. Eng. Des.*, **269**, 125-129.
- Srinivas, M. and Kamat, S.V. (1992), "Effect of notch root radius on ductile fracture toughness of Armco Iron", *Int. J. Fract. Mech.*, **58**, 15-21.
- Terán, G., Capula-Colindres, S., Angeles-Herrera, D., Velázquez, J.C. and Fernández-Cueto, M.J. (2016), "Estimation of fracture toughness kic from impact test data in t-welded connections repaired by grinding and wet welding", *Eng. Fract. Mech.*, **153**, 351-359.
- Tuba, F., Oláh, L. and Nagy, P. (2013), "On the valid ligament range of specimens for the essential work of fracture method: The inconsequence of stress criteria", *Eng. Fract. Mech.*, **99**, 349-355.
- Turner, C.E. (1984), "Methods for post-yield fracture safety assessment", Post-Yield Fracture Mechanics, Eds. Latzko. D.G.H, Turner. C.E., Landes. J.D., Mc Cabe. D.E. and Hellen. T.K., Elsevier, England.
- Witts, N.P. (2005), "Evaluation of the non linear fracture parameters J and C* wit ANSYS", Safe Consultancy, Leicester, UK.

CC

Nomenclature

K_V	Fracture energy	[J]
K_{IC}	Critical stress intensity factor	[MPa \sqrt{m}]
$J_{\rho C}$	Critical fracture toughness value	[MJ/m ²]
Γ_e	Specific essential work of fracture	[MJ/m ²]
J_C	Critical J integral	[MJ/m ²]
J_{IC}	Critical J-Integral Fracture toughness	[MJ/m ²]
J_ρ	Fracture toughness as a function of notch radius ρ .	[MJ/m ²]
$J\rho C$	Critical fracture toughness as a function of notch radius ρ .	[MJ/m ²]
U_t	total fracture work	[J]
U_e	essential work of fracture	[J]
U_{pl}	outer region work	[J]
σ_e	Yield limit stress	[MPa]
E	Young modulus	[MPa]
ρ	notch radius	[mm]
ρ_c	critical notch radius	[mm]
B	Specimen thickness	[mm]
a	Crack length	[mm]
W	specimen width	[mm]
a/W	Notch depth	
ψ	shape factor	
η	η factor	
F_{max}	Maximal force	[kN]
J_{ANSYS}	The computed values of J-integral	[MJ/m ²]